



Secrecy Analysis of Cooperative Vehicular Relaying Networks over Double-Rayleigh Fading Channels

Anshul Pandey¹ · Suneel Yadav¹

Published online: 4 June 2020

© Springer Science+Business Media, LLC, part of Springer Nature 2020

Abstract

In this paper, we investigate physical-layer security performance of the cooperative vehicular relaying networks, wherein the communication from a source vehicle to the destination vehicle is assisted by an amplify-and-forward (AF) relay vehicle in the presence of a passive eavesdropper vehicle. We assume that the communication links between the vehicles experience double-Rayleigh fading. We also consider two AF relaying protocols: (1) fixed gain relaying which requires partial channel state information (CSI), and (2) variable gain relaying which requires full CSI. Specifically, we derive the novel intercept probability and ergodic secrecy capacity expressions for both fixed and variable gain relaying in the presence of double-Rayleigh fading channels. The numerical and simulation results verify our theoretical and analytical findings, and show the impacts of channel conditions and relay and eavesdropper locations on the system secrecy performance.

Keywords Physical-layer security · Cooperative vehicular relaying networks · Intercept probability · Ergodic secrecy capacity · Double-Rayleigh fading channels

1 Introduction

Rapid proliferation of smart vehicles leveraged with wireless communication capabilities have allowed vehicular networks to support various exciting intelligent transportation system (ITS) applications such as, traffic management, payment services, and infotainment [1–3]. Moreover, coupling vehicular networks with cooperative relaying communications can enhance reliability, efficiency, and coverage of ITS applications and services [4–6]. Such relay assisted vehicular networks can be termed as cooperative vehicular relaying networks (CVRNs). Some traditional relaying protocols such as amplify-and-forward (AF) and decode-and-forward (DF) can be applied in such networks. The AF relaying protocol has attracted significant interest over DF protocol as it is easy to implement and

✉ Suneel Yadav
suneel@iiita.ac.in

Anshul Pandey
rse2016503@iiita.ac.in

¹ Department of Electronics and Communication Engineering, Indian Institute of Information Technology Allahabad, Prayagraj, Uttar Pradesh 211015, India

offers shorter latency. Moreover, based on the channel state information (CSI), it can operate under fixed gain relaying or variable gain relaying. In particular, the variable gain AF relaying requires instantaneous CSI, whereas the fixed gain relay needs only statistical CSI. Through vehicle-to-vehicle (V2V) and vehicle-to-infrastructure (V2I) modes of communication in CVRNs, information can be disseminated among the vehicles, roadside infrastructures, and users. Despite several advantages, such networks come with their own set of challenges, particularly in the domains of privacy and security [7–9]. Due to the inherent open nature of wireless medium, mobility, cooperativeness, and lack of central points, such networks are vulnerable to various security attacks [7] such as, eavesdropping, jamming, identity theft etc. Recently, there has been a growing interest for ensuring information security in CVRNs. Various upper-layer security mechanisms [9–11] are used to ensure the security in such networks. However, the dynamic nature of vehicular networks and lack of trusted central infrastructure entity can make the secret key distribution process vulnerable [12]. Moreover, such security mechanisms could become inefficient when the eavesdropper have the access to infinite computing capabilities. Amid these challenges, physical-layer security has emerged as an attractive option to compliment the existing cryptography based security infrastructure [13, 14]. It guarantees secure transmission by exploiting the inherent randomness of the wireless channel such as, fading, interferences etc. [15–17].

1.1 Related Works

Recently, physical-layer security in non-vehicular cooperative relaying networks have attracted considerable attention in the literature (see [18–26] and the references therein). However, all of them [18–26] are limited to the scenario where the nodes are stationary and the channel between the terminals can be distributed as Rayleigh fading or Nakagami- m fading. The authors in [27, 28] have investigated the secrecy performance of variable gain AF relay based CVRNs by considering the classical Rayleigh fading to model the V2V channel. However, cascaded fading models [29, 30] are found to be more appropriate to provide a realistic description of V2V channels, which can be produced by multiplying the channel gains of independent groups of scatterers around the mobile units. The performance of CVRNs by considering the cascaded channel modeling for V2V links have been investigated in [31–36]. Specifically, the authors in [31] have analyzed the performance of a multihop network under cascaded Rayleigh fading. The authors in [32] have evaluated the performance of DF-based multi-relay CVRNs under double-Rayleigh channels. In [33], the authors have investigated the performance of DF-based CVRN, where the end-to-end communication is assisted by both the mobile and fixed infrastructure units under mixed Rayleigh and double-Rayleigh fading. The authors in [34] have investigated the performance of CVRNs with variable gain AF relaying protocol under mixed Nakagami- m and double-Nakagami- m fading environment. Recently, the authors in [35] have analyzed the performance of a CVRN with incremental hybrid decode-amplify-and-forward relaying under double-Rayleigh fading. Further, the authors in [36] have evaluated the performance of fixed gain AF relay based CVRNs under cascaded Nakagami- m fading channels.

Although, these works [31–36] have investigated the performance of CVRNs, however, none of them has explored the security issues in CVRNs. So far, the open literature exploiting the physical-layer security aspects in the CVRNs is very limited [37–40]. The authors in [37] have evaluated the secrecy performance of non-cooperative vehicular networks under double-Rayleigh channels. In [38], the authors have evaluated the secrecy performance of DF-based CVRNs over double-Rayleigh fading channels. Very recently, the

authors in [39, 40] have evaluated the performance of cooperative variable gain AF-based vehicular network under mixed Rayleigh and double-Rayleigh fading environments.

1.2 Motivation

Extensive exploration and investigation on the physical-layer security aspects in securing non-vehicular relaying networks exist in the literature [18–26] and is still growing on. Such networks correspond to the scenario where the communicating terminals are stationary and the channel between them can be modeled as Rayleigh distributed or Nakagami- m distributed. The physical-layer security aspects in CVRNs systems have been well studied in [27, 28, 38–40]. In particular, the authors in [27, 28] have evaluated the physical-layer security aspects in CVRNs, however, the analysis was carried out by assuming classical Rayleigh fading for both V2V and V2I channels. Experimentally and theoretically, it is shown that V2V links are different from V2I links, and hence the cascaded channel models are found more suited for V2V links [29]. The authors in [38] have studied the secrecy performance of DF-based CVRNs in the presence of double-Rayleigh fading. Moreover, the authors in [39] have evaluated the secrecy performance of an AF-based CVRN by considering the relay and eavesdropper as vehicular terminals (channel between them is modeled as double-Rayleigh fading), and source and destination as the fixed infrastructure (channel between them is modeled as Rayleigh fading). Further, the authors in [40] have investigated the secrecy performance of AF-based CVRNs by considering source, relay, and eavesdropper as vehicles, and destination as the fixed terminal.

Therefore, based on the open literature and to the best of authors' knowledge, the secrecy analysis for AF-based CVRNs by considering all terminals as moving vehicle under both fixed and variable gain relaying in the presence of double-Rayleigh fading channels is yet to be investigated. Moreover, there is lack of performance evaluation measures, i.e., intercept probability and ergodic secrecy capacity (ESC) in terms of CVRNs with all vehicular communications links. Motivating ourselves from the above research gaps, we develop this treatise and want to fill these important research gaps.

1.3 Contributions

In this paper, we consider a dual-hop CVRN where the communication between a source vehicle and a destination vehicle is assisted by an AF relay vehicle in the presence of a passive eavesdropper vehicle. We consider two AF relaying strategies: (1) fixed gain relaying which requires partial CSI, and (2) variable gain relaying which requires full CSI. By modeling the vehicular communication links as double-Rayleigh fading channels, we derive the novel expressions for the intercept probability and ESC under both fixed and variable gain relaying of the considered system. With the help of numerical and simulation results, we corroborate our analytical findings. We further illustrate the effects of channel conditions and relay and eavesdropper locations on the system security performance. Our results reveal that the fixed gain AF relaying can achieve comparable secrecy performance to that of variable gain AF relaying protocol, without necessitating full CSI.

1.3.1 Notations

$\mathbb{E}[X]$ denotes the expectation of a random variable (RV) X . $F_X(\cdot)$ and $f_X(x)$ denote the cumulative distribution function (CDF) and probability density function (PDF) of X . $\mathcal{K}_\nu(\cdot)$ denotes the

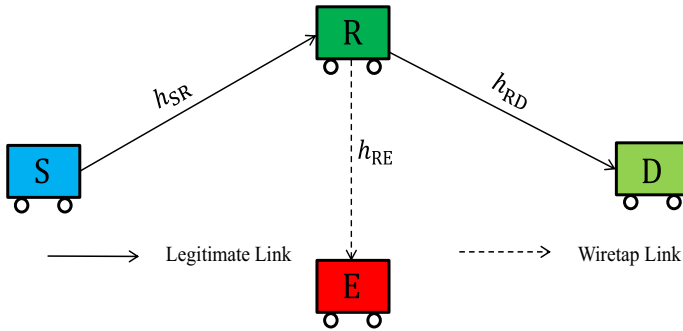


Fig. 1 System model for secure cooperative vehicular relaying network

ν -th order modified Bessel function of second kind [41, Eq. (8.432)], $G_{p,q}^{m,n}(x|_{b_1, \dots, b_q}^{a_1, \dots, a_p})$ is the Meijer-G function [41, Eq. (9.301)], ${}_2F_1(\cdot, \cdot; \cdot; \cdot)$ is the hypergeometric function [41, Eq. (9.111)], $G_{p_1, q_1; p_2, q_2; p_3, q_3}^{m_1, n_1; m_2, n_2; m_3, n_3}(x, y|_{b_1, \dots, b_{q_1}}^{a_1, \dots, a_{p_1}}|_{d_1, \dots, d_{q_2}}^{c_1, \dots, c_{p_2}}|_{f_1, \dots, f_{q_3}}^{e_1, \dots, e_{p_3}})$ is the extended generalized bivariate Meijer-G function [42, Eq. (07.34.21.0081.01)], $\Psi(\cdot)$ denotes the psi function [41, Eq. (8.360.1)], and $\Gamma(\cdot)$ denotes the complete gamma function [41, Eq. (8.350)].

2 System and Channel Models

We consider a secure CVRN (as shown in Fig. 1), in which a legitimate source vehicle S communicates with the legitimate destination vehicle D by the assistance of an AF relay vehicle R in the presence of a passive eavesdropper vehicle E. All vehicles are equipped with a single antenna. The direct links between S and D, and S and E are absent due to the heavy path-loss and shadowing. We assume that all channels are assumed to be quasi-static, reciprocal, and subject to independent and non-identically distributed (i.i.d.) double-Rayleigh fading. In particular, the channel coefficients h_{ij} for $\{ij\} \in \{SR, RD, RE\}$ can be modeled as the product of $h_{ij,1}$ and $h_{ij,2}$, where $h_{ij,1}$ and $h_{ij,2}$ are independent complex Gaussian random variables (RVs) having zero mean and variance $\Omega_{ij,1}$ and $\Omega_{ij,2}$, respectively. We also assume the additive white Gaussian noise (AWGN) with zero mean and N_0 variance for each link.

The communication from S to D in the presence of a passive E will be accomplished via R in two transmission phases. In the first transmission phase, S transmits its unit energy signal x_s with power P_s . The signal received at R can be expressed as $y_r = \sqrt{P_s}h_{SR}x_s + n_r$, where n_r is the AWGN at R. During the second transmission phase, R amplifies the received signal y_r with some amplification factor \mathcal{G} , and the signal received at D and E can be given, respectively, as

$$y_d = \mathcal{G}h_{RD} \left(\sqrt{P_s}h_{SR}x_s + n_r \right) + n_d, \tag{1}$$

$$y_e = \mathcal{G}h_{RE} \left(\sqrt{P_s}h_{SR}x_s + n_r \right) + n_e, \tag{2}$$

where n_d and n_e are the AWGNs at D and E, and the amplification factor \mathcal{G} is selected at R to satisfy its power constraint. If R has instantaneous knowledge of the fading channel, h_{SR} , it can apply variable gain relaying with $\mathcal{G}^v = \sqrt{\frac{P_r}{E_{x_s, n_r} \{|y_r|\}^2}}$, where P_r denotes the relay

power. Otherwise, fixed gain relaying (using only statistical CSI) with $\mathcal{G}^f = \sqrt{\frac{P_r}{\mathbb{E}_{x_s, h_{SR}, n_r} \{|y_r|\}^2}}$ can be employed. For the fixed and variable gain relaying, the amplification factor \mathcal{G} can be considered as

$$\mathcal{G}^f = \sqrt{\frac{P_r}{P_s \mathbb{E}_{|h_{SR}|^2} \{|h_{SR}|^2\} + N_0}}, \tag{3}$$

$$\mathcal{G}^v = \sqrt{\frac{P_r}{P_s |h_{SR}|^2 + N_0}}, \tag{4}$$

respectively. Further, using the expressions \mathcal{G}^f and \mathcal{G}^v , and after some algebraic manipulations, we can express the instantaneous end-to-end signal-to-noise ratios (SNRs) at D and E for the fixed gain relaying as

$$\Lambda_D^f = \frac{\lambda_{SR} \lambda_{RD}}{C + \lambda_{RD}} \quad \text{and} \quad \Lambda_E^f = \frac{\lambda_{SR} \lambda_{RE}}{C + \lambda_{RE}}, \tag{5}$$

and for the variable gain relaying as

$$\Lambda_D^v = \frac{\lambda_{SR} \lambda_{RD}}{\lambda_{SR} + \lambda_{RD} + 1} \quad \text{and} \quad \Lambda_E^v = \frac{\lambda_{SR} \lambda_{RE}}{\lambda_{SR} + \lambda_{RE} + 1}, \tag{6}$$

where $\lambda_{SR} = \frac{P_s}{N_0} |h_{SR}|^2$, $\lambda_{RD} = \frac{P_r}{N_0} |h_{RD}|^2$, $\lambda_{RE} = \frac{P_r}{N_0} |h_{RE}|^2$, and $C = \frac{P_r}{N_0 (\mathcal{G}^f)^2}$ is a constant for fixed \mathcal{G}^f .

Moreover, the capacities pertaining to $S \rightarrow R \rightarrow D$ and $S \rightarrow R \rightarrow E$ links of the considered system can be defined as $C_D^b = \frac{1}{2} \log_2(1 + \Lambda_D^b)$ and $C_E^b = \frac{1}{2} \log_2(1 + \Lambda_E^b)$, for $b = \{ f, v \}$, respectively.

Thus, the secrecy capacity of the considered system can be expressed as

$$C_{SEC}^b = \max \{ C_D^b - C_E^b, 0 \}, \tag{7}$$

where $b = \{ f, v \}$.

3 Performance Analysis

Here, we analyze the intercept probability and ergodic secrecy capacity (ESC) of the considered system for fixed and variable gain relaying under double-Rayleigh fading channels. Note that h_{ij} for $\{ij\} \in \{SR, RD, RE\}$ is distributed as double-Rayleigh fading, therefore, the CDF and PDF for the channel gain $|h_{ij}|^2$ are given as $F_{|h_{ij}|^2}(x) = 1 - (2/\Omega_{ij}) \sqrt{x} \mathcal{K}_1((2/\Omega_{ij}) \sqrt{x})$, $x > 0$ and $f_{|h_{ij}|^2}(x) = (2/\Omega_{ij}^2) \mathcal{K}_0((2/\Omega_{ij}) \sqrt{x})$, $x > 0$, (assuming $\Omega_{ij,1} = \Omega_{ij,2} = \Omega_{ij}$) respectively. This will help us to conduct the analytical derivation of performance metrics under investigation in what follows.

3.1 Intercept Probability

The intercept probability is an important performance measure used to evaluate the secrecy performance of cooperative relaying networks. It is defined as the probability that the eavesdropper succeeds to intercept the signal forwarded for the legitimate receiver or in other words, the secrecy capacity falls below zero [18]. Mathematically, for the considered system under fixed and variable gain relaying, it can be written as

$$\mathcal{P}_{\text{int}}^b = \Pr \left[C_D^b - C_E^b < 0 \right], \tag{8}$$

where $b = \{ f, v \}$.

3.1.1 Fixed Gain Relaying

For fixed gain relaying scenario, the intercept probability of the considered system can be expressed as

$$\begin{aligned} \mathcal{P}_{\text{int}}^f &= \Pr \left[C_D^f - C_E^f < 0 \right] \\ &= \Pr \left[A_D^f - A_E^f < 0 \right] \\ &= \Pr \left[\frac{\lambda_{\text{SR}} \lambda_{\text{RD}}}{C + \lambda_{\text{RD}}} < \frac{\lambda_{\text{SR}} \lambda_{\text{RE}}}{C + \lambda_{\text{RE}}} \right], \end{aligned} \tag{9}$$

which after some simplifications can be expressed as

$$\begin{aligned} \mathcal{P}_{\text{int}}^f &= \Pr \left[\lambda_{\text{RD}} < \lambda_{\text{RE}} \right] \\ &= \int_0^\infty F_{\lambda_{\text{RD}}}(y) f_{\lambda_{\text{RE}}}(y) dy. \end{aligned} \tag{10}$$

Invoking the CDF of λ_{RD} and the PDF of λ_{RE} into (10), $\mathcal{P}_{\text{int}}^f$ can be expressed as

$$\mathcal{P}_{\text{int}}^f = \int_0^\infty \left(1 - 2\alpha_{\text{RD}} \sqrt{y} \mathcal{K}_1(2\alpha_{\text{RD}} \sqrt{y}) \right) 2\alpha_{\text{RE}}^2 \mathcal{K}_0(2\alpha_{\text{RE}} \sqrt{y}) dy. \tag{11}$$

Further, making the change of variable $y = t^2$ within the integral and then using [41, Eq. (6.576.4)], we can obtain the intercept probability under fixed gain relaying, $\mathcal{P}_{\text{int}}^f$, as

$$\mathcal{P}_{\text{int}}^f = 1 - \frac{\alpha_{\text{RE}}^2}{2\alpha_{\text{RD}}^2} \Gamma(2, 2, 1, 1) {}_2F_1 \left(2, 1; 3; 1 - \frac{\alpha_{\text{RE}}^2}{\alpha_{\text{RD}}^2} \right), \tag{12}$$

where $\alpha_{\text{RD}} = \frac{\sqrt{N_0}}{\sqrt{P_r \Omega_{\text{RD}}}}$, $\alpha_{\text{RE}} = \frac{\sqrt{N_0}}{\sqrt{P_r \Omega_{\text{RE}}}}$, and $\Gamma(a_1, \dots, a_p) = \prod_{k=1}^p \Gamma(a_k)$.

We can see from (12) that the intercept probability expression involves powers, incomplete gamma function, and hypergeometric function containing the transmit powers and average channel gains, which can be easily calculated via software packages such as Matlab or Mathematica.

3.1.2 Variable Gain Relaying

Under variable gain relaying scenario, the intercept probability of the considered system can be given by

$$\begin{aligned} \mathcal{P}_{\text{int}}^v &= \Pr[C_D^v - C_E^v < 0] \\ &= \Pr[A_D^v - A_E^v < 0]. \end{aligned} \tag{13}$$

With the fact that $\frac{XY}{X+Y} < \min(X, Y)$, the A_D^v and A_E^v can be tightly upper bounded as $A_D^v < \min(\lambda_{\text{SR}}, \lambda_{\text{RD}})$ and $A_E^v < \min(\lambda_{\text{SR}}, \lambda_{\text{RE}})$. However, it is noted that such an upper bound can be treated as tight approximation over the entire range of operating SNR. Consequently, we can express (13) as

$$\mathcal{P}_{\text{int}}^v \approx \int_0^\infty F_{A_D^v}(y) f_{A_E^v}(y) dy, \tag{14}$$

where

$$\begin{aligned} F_{A_D^v}(x) &= \Pr[\min(\lambda_{\text{SR}}, \lambda_{\text{RD}}) < x] \\ &= F_{\lambda_{\text{SR}}}(x) + F_{\lambda_{\text{RD}}}(x) - F_{\lambda_{\text{SR}}}(x)F_{\lambda_{\text{RD}}}(x) \\ &= 1 - 4\alpha_{\text{SR}}\alpha_{\text{RD}}x\mathcal{K}_1(2\alpha_{\text{SR}}\sqrt{x})\mathcal{K}_1(2\alpha_{\text{RD}}\sqrt{x}), \end{aligned} \tag{15}$$

$$\begin{aligned} f_{A_E^v}(x) &= \frac{\partial}{\partial x} \{ \Pr[\min(\lambda_{\text{SR}}, \lambda_{\text{RE}}) < x] \} \\ &= 4\alpha_{\text{SR}}^2\alpha_{\text{RE}}\sqrt{x}\mathcal{K}_0(2\alpha_{\text{SR}}\sqrt{x})\mathcal{K}_1(2\alpha_{\text{RE}}\sqrt{x}) \\ &\quad + 4\alpha_{\text{SR}}\alpha_{\text{RE}}^2\sqrt{x}\mathcal{K}_1(2\alpha_{\text{SR}}\sqrt{x})\mathcal{K}_0(2\alpha_{\text{RE}}\sqrt{x}), \end{aligned} \tag{16}$$

where we have used the fact that $\frac{\partial^n}{\partial x^n} [x^{\frac{v}{2}}\mathcal{K}_v(ax\sqrt{x})] = (-\frac{a}{2})^n x^{\frac{(v-n)}{2}}\mathcal{K}_{v-n}(ax\sqrt{x})$ [43, Eq. (1.14.1.4)] to obtain the second equality in (16), and $\alpha_{\text{SR}} = \frac{\sqrt{N_0}}{\sqrt{P_s}\Omega_{\text{SR}}}$.

Now, invoking (15) and (16) into (14), and after evaluating the required integrals, the intercept probability under variable gain relaying can be obtained as per following theorem.

Theorem 1 *The intercept probability for variable gain relaying scenario under double-Rayleigh fading channels can be expressed as*

$$\begin{aligned} \mathcal{P}_{\text{int}}^v &= 1 - \frac{\sqrt{\pi}}{2} \frac{\alpha_{\text{SR}}\alpha_{\text{RE}}}{\alpha_{\text{RD}}^2} G_{4,2:0,2:2,0}^{-0,4;2,0:2,0} \left(\begin{matrix} -0.5, -0.5, 0.5, 0.5 \\ 0, -0.5 \end{matrix} \middle| \begin{matrix} 2, 1 \\ 0.5, -0.5 \end{matrix} \middle| \frac{\alpha_{\text{RD}}^2}{4\alpha_{\text{SR}}^2}, \frac{\alpha_{\text{RE}}^2}{4\alpha_{\text{SR}}^2} \right) \\ &\quad - \frac{\sqrt{\pi}}{2} \frac{\alpha_{\text{RE}}^2}{\alpha_{\text{RD}}^2} G_{3,1:0,2:2,0}^{-0,3;2,0:2,0} \left(\begin{matrix} 0, -1, 1 \\ -0.5 \end{matrix} \middle| \begin{matrix} 2, 1 \\ 0, 0 \end{matrix} \middle| \frac{\alpha_{\text{RD}}^2}{4\alpha_{\text{SR}}^2}, \frac{\alpha_{\text{RE}}^2}{4\alpha_{\text{SR}}^2} \right). \end{aligned} \tag{17}$$

Proof See “Appendix 1” for the proof. □

It can be observed from (17) that the intercept probability expression involves powers and extended generalized bivariate Meijer-G functions containing the transmit powers

and average channel gains, which can be easily evaluated using the Matlab or Mathematica softwares.

3.2 Ergodic Secrecy Capacity (ESC)

It can be easily observed from (7) that the achievable secrecy capacity $C_{SEC}^b = 0$ when $C_D^b \leq C_E^b$, for $b = \{f, v\}$, therefore, the secrecy capacity can only be achieved for the case when $C_D^b > C_E^b$. Consequently, the ESC for the considered system under fixed and variable gain relaying can be mathematically expressed as

$$\begin{aligned} \bar{C}_{SEC}^b &= \mathbb{E} \left[C_D^b - C_E^b \right] \\ &= \frac{1}{2} \mathbb{E} \left[\log_2 \left(1 + \lambda_D^b \right) \right] - \frac{1}{2} \mathbb{E} \left[\log_2 \left(1 + \lambda_E^b \right) \right], \end{aligned} \tag{18}$$

where $b = \{f, v\}$.

3.2.1 Fixed Gain Relaying

Under fixed gain relaying scenario, the ESC using (5) and (18) can be expressed as

$$\begin{aligned} \bar{C}_{SEC}^f &= \frac{1}{2} \left\{ \mathbb{E} \left[\log_2 \left(1 + \frac{\lambda_{SR} \lambda_{RD}}{C + \lambda_{RD}} \right) \right] - \mathbb{E} \left[\log_2 \left(1 + \frac{\lambda_{SR} \lambda_{RE}}{C + \lambda_{RE}} \right) \right] \right\} \\ &= \frac{1}{2 \ln(2)} \left\{ \underbrace{\mathbb{E} \left[\ln \left(1 + \frac{\lambda_{SR} \lambda_{RD}}{C + \lambda_{RD}} \right) \right]}_{\triangleq \bar{C}_D^f} - \underbrace{\mathbb{E} \left[\ln \left(1 + \frac{\lambda_{SR} \lambda_{RE}}{C + \lambda_{RE}} \right) \right]}_{\triangleq \bar{C}_E^f} \right\}, \end{aligned} \tag{19}$$

which can be then evaluated and presented in the following theorem.

Theorem 2 For the fixed gain relaying, the ESC can be obtained as

$$\begin{aligned} \bar{C}_{SEC}^f &= \frac{1}{2 \ln(2)} \left\{ \alpha_{SR}^2 \alpha_{RD}^2 C \sum_{k=0}^{\infty} \frac{1}{k!} \left(\frac{-1}{C \alpha_{RD}^2} \right)^k G_{3,7}^{6,2} \left(\alpha_{SR}^2 \alpha_{RD}^2 C \middle|_{0,0,k,k,k-1,k-1,k}^{0,k-1,k} \right) \right. \\ &\quad - G_{4,2}^{1,4} \left(\frac{1}{\alpha_{RD}^2 C} \middle|_{1,0}^{0,0,1,1} \right) + G_{4,2}^{1,4} \left(\frac{1}{\alpha_{RE}^2 C} \middle|_{1,0}^{0,0,1,1} \right) \\ &\quad \left. - \alpha_{SR}^2 \alpha_{RE}^2 C \sum_{k=0}^{\infty} \frac{1}{k!} \left(\frac{-1}{C \alpha_{RE}^2} \right)^k G_{3,7}^{6,2} \left(\alpha_{SR}^2 \alpha_{RE}^2 C \middle|_{0,0,k,k,k-1,k-1,k}^{0,k-1,k} \right) \right\}. \end{aligned} \tag{20}$$

Proof See “Appendix 2” for the detailed derivation. □

The expression in (20) can be easily evaluated via Matlab or Mathematica softwares. It is also worth mentioning that (20) contains the infinite series expansion, which converges fast as shown numerically in Sect. 4.

3.2.2 Variable Gain Relaying

Under variable gain relaying scenario, the ESC of the considered system is presented in Theorem 3.

Theorem 3 For variable gain relaying scenario, the ESC can be given by

$$\bar{C}_{SEC}^v = \frac{1}{2 \ln(2)} [\mathcal{T}_1 - \mathcal{T}_2 - \mathcal{T}_3 + \mathcal{T}_4], \tag{21}$$

where

$$\mathcal{T}_1 = \xi_1 \left(\frac{1}{\alpha_{RD}^2} \right), \tag{22}$$

$$\mathcal{T}_2 = \xi_1 \left(\frac{1}{\alpha_{RE}^2} \right), \tag{23}$$

$$\begin{aligned} \mathcal{T}_3 = & \xi_1 \left(\frac{M}{\alpha_{RD}^2} \right) - \frac{\alpha_{RD}^2}{M} \xi_2 \left(1, 0, 0, 0, \alpha_{SR}^2, \frac{\alpha_{RD}^2}{M} \right) + \xi_1 \left(\frac{1}{\alpha_{SR}^2} \right) \\ & - \alpha_{SR}^2 \xi_2 \left(0, 0, 1, 0, \alpha_{SR}^2, \frac{\alpha_{RD}^2}{M} \right) + \sum_{k=2}^M \left\{ -\xi_1 \left(\frac{1}{\alpha_{RD}^2 \tau_{k-1}} \right) + \xi_1 \left(\frac{1}{\alpha_{RD}^2 \tau_k} \right) \right. \\ & + \alpha_{SR} \alpha_{RD} \sqrt{(1 - \tau_{k-1}) \tau_{k-1}} \xi_2 \left(0.5, 0.5, 0.5, -0.5, \alpha_{SR}^2 (1 - \tau_{k-1}), \alpha_{RD}^2 \tau_{k-1} \right) \\ & + \alpha_{RD}^2 \tau_{k-1} \xi_2 \left(1, 0, 0, 0, \alpha_{SR}^2 (1 - \tau_{k-1}), \alpha_{RD}^2 \tau_{k-1} \right) \\ & \left. - \alpha_{RD}^2 \tau_k \xi_2 \left(1, 0, 0, 0, \alpha_{SR}^2 (1 - \tau_{k-1}), \alpha_{RD}^2 \tau_k \right) - \alpha_{SR} \alpha_{RD} \sqrt{(1 - \tau_{k-1}) \tau_k} \right. \\ & \left. \times \xi_2 \left(0.5, 0.5, 0.5, -0.5, \alpha_{SR}^2 (1 - \tau_{k-1}), \alpha_{RD}^2 \tau_{k-1} \right) \right\}, \tag{24} \end{aligned}$$

$$\begin{aligned} \mathcal{T}_4 = & \xi_1 \left(\frac{M}{\alpha_{RE}^2} \right) - \frac{\alpha_{RE}^2}{M} \xi_2 \left(1, 0, 0, 0, \alpha_{SR}^2, \frac{\alpha_{RE}^2}{M} \right) + \xi_1 \left(\frac{1}{\alpha_{SR}^2} \right) \\ & - \alpha_{SR}^2 \xi_2 \left(0, 0, 1, 0, \alpha_{SR}^2, \frac{\alpha_{RE}^2}{M} \right) + \sum_{k=2}^M \left\{ -\xi_1 \left(\frac{1}{\alpha_{RE}^2 \tau_{k-1}} \right) + \xi_1 \left(\frac{1}{\alpha_{RE}^2 \tau_k} \right) \right. \\ & + \alpha_{SR} \alpha_{RE} \sqrt{(1 - \tau_{k-1}) \tau_{k-1}} \xi_2 \left(0.5, 0.5, 0.5, -0.5, \alpha_{SR}^2 (1 - \tau_{k-1}), \alpha_{RE}^2 \tau_{k-1} \right) \\ & + \alpha_{RE}^2 \tau_{k-1} \xi_2 \left(1, 0, 0, 0, \alpha_{SR}^2 (1 - \tau_{k-1}), \alpha_{RE}^2 \tau_{k-1} \right) \\ & \left. - \alpha_{RE}^2 \tau_k \xi_2 \left(1, 0, 0, 0, \alpha_{SR}^2 (1 - \tau_{k-1}), \alpha_{RE}^2 \tau_k \right) - \alpha_{SR} \alpha_{RE} \sqrt{(1 - \tau_{k-1}) \tau_k} \right. \\ & \left. \times \xi_2 \left(0.5, 0.5, 0.5, -0.5, \alpha_{SR}^2 (1 - \tau_{k-1}), \alpha_{RE}^2 \tau_{k-1} \right) \right\}, \tag{25} \end{aligned}$$

$$\xi_1(a) = G_{4,2}^{1,4}(a|_{1,0}^{0,0,1,1}), \tag{26}$$

$$\xi_2(a, b, c, d, e, f) = G_{2,2:0,2:0,2}^{2,1:2,0:2,0}(-1,0|_{-1,-1}|_{a,b}|_{c,d}|e,f), \tag{27}$$

with $\tau_k = \frac{k}{M}$ and $\tau_{k-1} = \frac{k-1}{M}$.

Proof The proof is given in “Appendix 3”. □

The ESC expression under variable gain relaying consists of finite summations with powers, Meijer-*G* functions, and extended generalized bivariate Meijer-*G* functions consisting of transmit powers and average channel gains, which can be evaluated via Matlab or Mathematica software packages.

4 Numerical Results and Discussion

In this section, we provide our derived analytical results for intercept probability and ESC for the considered system under fixed and variable gain relaying protocols with the help of numerical results (using Mathematica) and Monte-Carlo simulations (using Matlab). We consider a path-loss model with an exponent of four. Without loss of generality, we denote d_{ij} as the distance between the nodes i and j , where $ij \in \{SR, RD, RE\}$. We also consider a normalized square area (a two dimensional network topology), where the coordinates of node S, R, D, and E are $(0, 0)$, $(x_R, 0)$, $(1, 0)$, and (x_E, y_E) , respectively. Accordingly, we have $d_{SR} = x_R$, $d_{RD} = 1 - x_R$, and $d_{RE} = \sqrt{(x_R - x_E)^2 + y_E^2}$. Let the mean values of the average channel gains of the links $S \rightarrow R$, $R \rightarrow D$, and $R \rightarrow E$ are denoted by γ_{SR} , γ_{RD} , and γ_{RE} , respectively, and the main-to-eavesdropper ratio (MER) for the relay link is given as $\lambda = \frac{\gamma_{RD}}{\gamma_{RE}}$. Accordingly, the average channel gain between the nodes i and j is set to $\Omega_{ij} = d_{ij}^{-4} \lambda_{ij}$, where $ij \in \{SR, RD, RE\}$. We set $\gamma_{SR} = \gamma_{RD} = 1$ and $\gamma_{RE} = \frac{1}{\lambda}$. We also assume $P_s = P_r = P$ and $\rho = \frac{P}{N_0}$.

Figures 2 and 3 depict the intercept probability performance of the considered system as a function of MER under fixed and variable gain AF relaying strategies, respectively, for different eavesdropper locations (i.e., x_E and y_E) when $\rho = 10$ dB. As can be seen from Figs. 2 and 3 that the derived analytical expressions of intercept probability for fixed and variable gain relaying are matched perfectly with the simulation results over the entire MER regime. This validates the correctness of the derived analytical expressions. Also, we can observe that the system intercept probability decreases as λ increases for fixed and variable gain relaying. This is due to the fact that with the increase in MER (λ), $R \rightarrow E$ link quality worsens compared to $R \rightarrow D$ link quality. In addition, it is also seen that a shorter $R \rightarrow E$ link (small d_{RE}) improves the eavesdropper ability to intercept, which is because of the fact that the shorter d_{RE} helps in strengthening the quality of wiretap $R \rightarrow E$ link. Moreover, one can observe from Figs. 2 and 3 that the intercept probability of fixed gain relaying is nearer to that of variable gain relaying. Thus, the fixed gain relaying can bring almost comparable intercept probability performance to variable gain relaying, without the need for full CSI.

Figure 4 plots the ESC versus MER for both fixed and variable gain relaying strategies for various values of x_E and y_E , when $M = 20$ and $\rho = 10$ dB. It can be seen from the plots

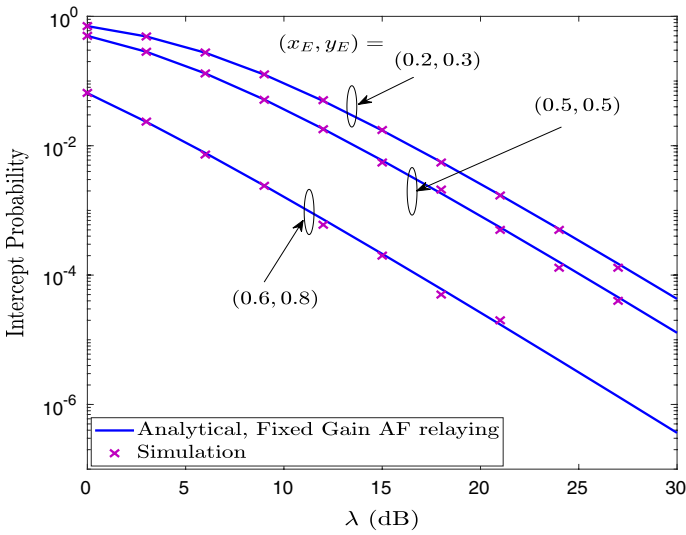


Fig. 2 Intercept probability versus MER with fixed gain AF relaying

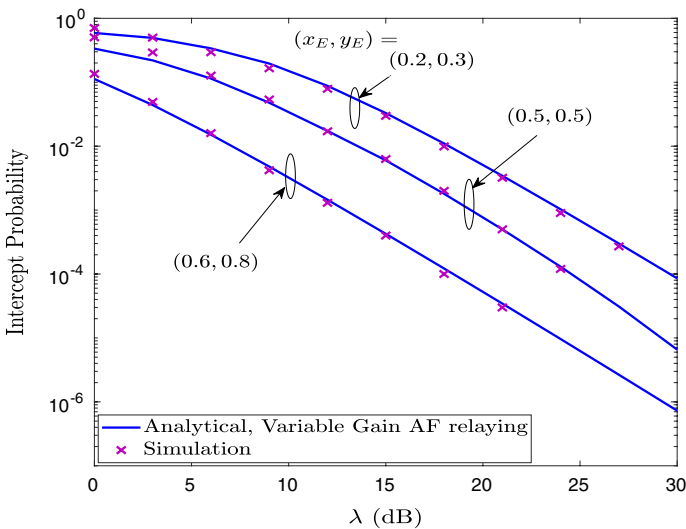


Fig. 3 Intercept probability versus MER with variable gain AF relaying

that the derived analytical ESC results for both fixed and variable gain relaying are in good agreement with the simulation results over the entire range of operating MER. The analytical curves for ESC under variable gain relaying are obtained by truncating the infinite series expansion over index k in (20) to first few terms. As expected, the ESC performance under both relaying scenarios improves with increase in MER, irrespective of the eavesdropper location. This is owing to the better $R \rightarrow D$ link quality than $R \rightarrow E$ link quality. However, the ESC curves saturate in the high MER regime as ESC grows logarithmically

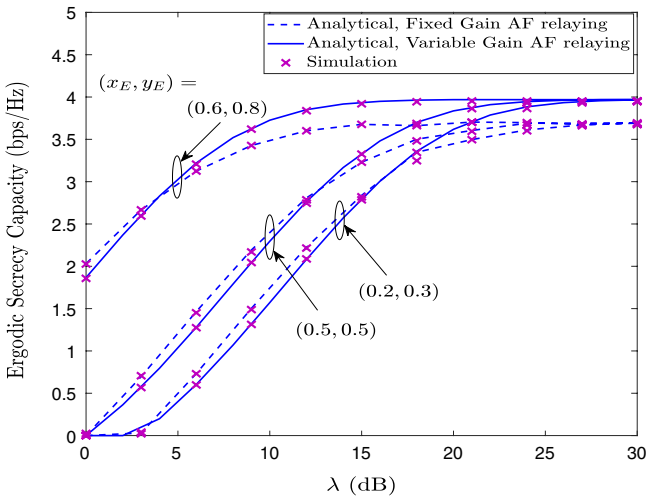


Fig. 4 ESC versus λ for different eavesdropper locations

with MER. Also, the ESC performance of the considered system under both the strategies degrades as d_{RE} shortens. This is because of the reason that a shorter d_{RE} results into a better wiretap channel quality. For instance, for variable gain AF (fixed gain AF) strategy with $\lambda = 18$ dB, when $(x_E, y_E) = (0.5, 0.5)$ so that $d_{RE} = 0.50$, the ESC is 3.70076 bps/Hz (3.4815 bps/Hz), while for $(x_E, y_E) = (0.6, 0.8)$ so that $d_{RE} = 0.806$, the ESC is 0.3.96311 bps/Hz (3.6620 bps/Hz). Further, we can observe that the variable gain relaying provides a slightly better ESC performance in the medium-to-high MER than the fixed gain AF relaying.

Figure 5 illustrates the impact of relay-to-eavesdropper distance, d_{RE} upon ESC performance under both the relaying schemes for different values of λ , when $M = 20$, $x_R = x_E = 0.5$, and $\rho = 10$ dB. Also, we have $d_{RE} = \sqrt{(x_E - 0.5)^2 + y_E^2}$ and y_E moves from 0.1 to 3 (corresponding to d_{RE} from 0.1 to 3). As can be seen from the Fig. 5 that the ESC performance under both fixed and variable gain relaying improves with the increase in d_{RE} , irrespective of λ . This is owing to the reason that as d_{RE} increases, R \rightarrow E link quality becomes poorer. Further, we can see that the ESC performance improves under both the relaying strategies as MER increases. This improvement in the ESC performance is because of the reason that the legitimated channel quality improves with the increase in MER. Also, we can see that the variable gain relaying provides a slightly better ESC performance than the fixed gain AF relaying for medium-to-high values of d_{RE} . For low values of d_{RE} , fixed gain AF relaying can achieve a marginally better ESC performance to that of variable gain AF relay. Therefore, we can see from Figs. 4 and 5 that fixed gain relaying can provide comparable ESC performance to that of variable gain AF relay strategy.

Figures 6 and 7 illustrate the impact of relay location on the ESC performance under both the relaying strategies, for various values of x_E and y_E , when $M = 20$, $\rho = 10$ dB, and $\lambda = 10$ dB. From the plots for the fixed gain relaying in Fig. 6, it can be seen that the relay location for maximum ESC is affected by the R \rightarrow E link only. In particular, from the plots of Fig. 6, it can be observed that when $x_E > 0.5$ and $y_E \leq 0.5$, the ESC achieves

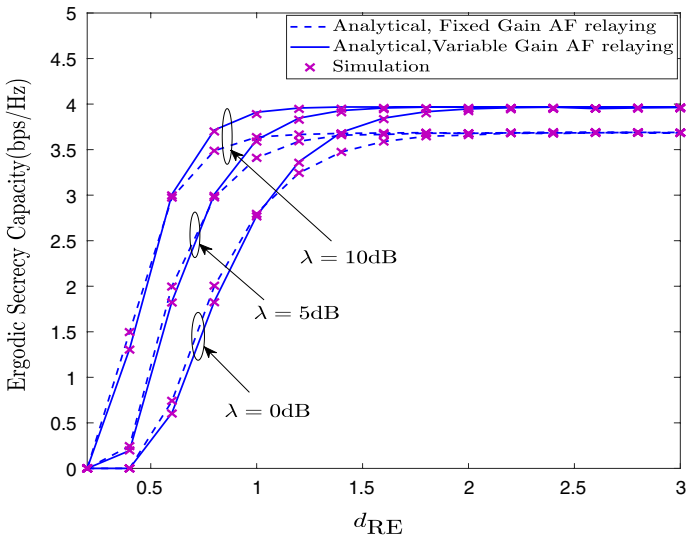


Fig. 5 Impact of relay-to-eavesdropper distance on the ESC performance

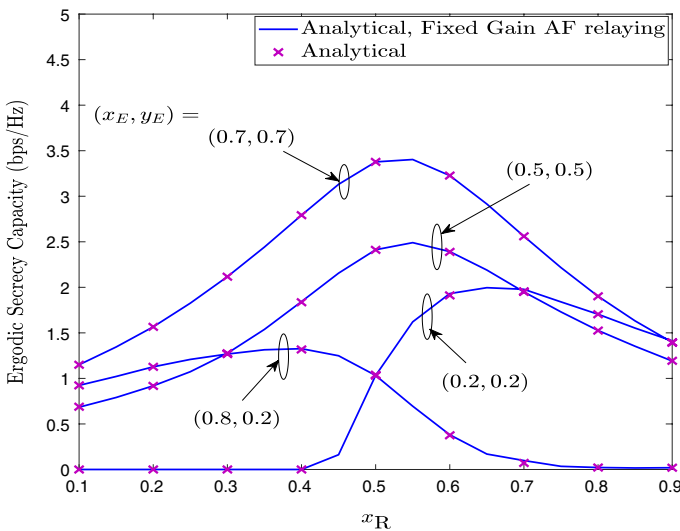


Fig. 6 Impact of relay location on the ESC performance under fixed gain relaying

a maximum value for relay location x_R^1 i.e., $x_R^* \leq 0.5$, whereas for $x_E < 0.5$ and $y_E \leq 0.5$, the maximum ESC occurs at $x_R^* \geq 0.5$. For instance, when $x_E = 0.2, y_E = 0.2$, the maximum ESC occurs at $x_R^* = 0.65$, whereas for $x_E = 0.8$ and $y_E = 0.2$, it occurs at $x_R^* = 0.40$.

¹ Note that x_R^* can be evaluated by numerically solving the optimization problem using the software packages such as Matlab and Mathematica.

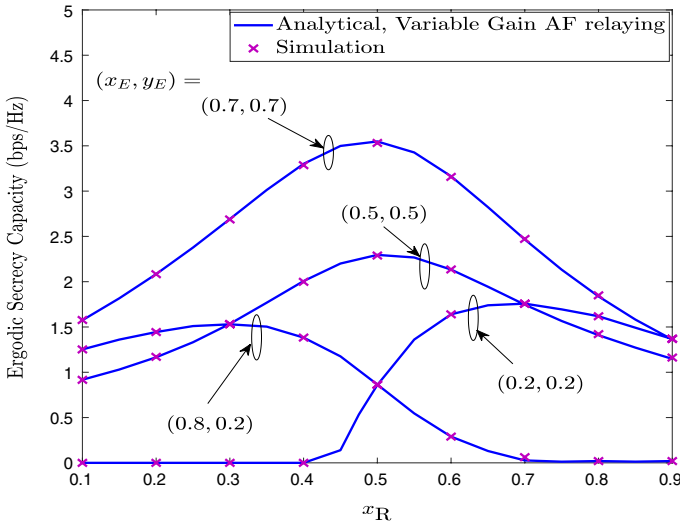


Fig. 7 Impact of relay location on the ESC performance under variable gain relaying

Similarly, under variable gain relaying in Fig. 7, we can observe that when $x_E > 0.5$ and $y_E \leq 0.5$, maximum ESC value occurs for $x_R^* \leq 0.5$, whereas for $x_E < 0.5$ and $y_E \leq 0.5$, the maximum ESC occurs at $x_R^* \geq 0.5$.

5 Conclusion

We evaluated the secrecy performance of a CVRN where a source vehicle communicates with a destination vehicle by the assistance of an AF relay vehicle in the presence of a passive eavesdropper vehicle. By considering both fixed and variable gain AF relaying protocols, we deduced the new expressions for the intercept probability and ESC of the considered system under double-Rayleigh fading channels. The analytical findings were corroborated with the help of numerical and simulation results. We have also examined the impacts of channel conditions and relay and eavesdropper locations on the secrecy performance. From a practical standpoint, our results also revealed that the fixed gain relaying can bring a comparable intercept probability and ESC performances to variable gain relaying, without requiring full CSI. Therefore, the fixed gain relaying can be an attractive option in CVRNs due to its ease in implementation and reduced complexity.

Acknowledgements This research work was supported by the Science and Engineering Research Board (a statutory body of the DST, Govt. of India), under Project ECR/2017/000104.

Appendix 1: Proof of Theorem 1

Using (14), (15), and (16), and after some simplifications, we can express $\mathcal{P}_{\text{int}}^v$ under double-Rayleigh fading channels as

$$\begin{aligned}
 \mathcal{P}_{\text{int}}^v &= 1 - 16\alpha_{\text{RE}}\alpha_{\text{RD}}\alpha_{\text{SR}}^3 \\
 &\quad \times \underbrace{\int_0^\infty x^{3/2}\mathcal{K}_1(2\alpha_{\text{SR}}\sqrt{x})\mathcal{K}_0(2\alpha_{\text{SR}}\sqrt{x})\mathcal{K}_1(2\alpha_{\text{RD}}\sqrt{x})\mathcal{K}_1(2\alpha_{\text{RE}}\sqrt{x})dx}_{\triangleq \mathcal{I}_1} \\
 &\quad - 16\alpha_{\text{RE}}^2\alpha_{\text{RD}}\alpha_{\text{SR}}^2 \underbrace{\int_0^\infty x^{3/2}(\mathcal{K}_1(2\alpha_{\text{SR}}\sqrt{x}))^2\mathcal{K}_0(2\alpha_{\text{RE}}\sqrt{x})\mathcal{K}_1(2\alpha_{\text{RD}}\sqrt{x})dx}_{\triangleq \mathcal{I}_2}.
 \end{aligned}
 \tag{28}$$

By applying the facts that $(b\sqrt{x})^\alpha\mathcal{K}_\beta(b\sqrt{x}) = 2^{\alpha-1}\mathcal{G}_{0,2}^{2,0}\left(\frac{(b\sqrt{x})^2}{4}\middle|\frac{\alpha+\beta}{2},\frac{\alpha-\beta}{2}\right)$ [44, p. 54], $\mathcal{K}_\alpha(a\sqrt{x})\mathcal{K}_\beta(a\sqrt{x}) = \frac{\sqrt{\pi}}{2}\mathcal{G}_{2,4}^{4,0}\left(a^2x\middle|\frac{\alpha+\beta}{2},\frac{\alpha-\beta}{2},\frac{-\alpha+\beta}{2},\frac{-\alpha-\beta}{2}\right)$ [45, Eq. (8.4.23.31)], and $\mathcal{K}_\alpha(\sqrt{x}) = \frac{1}{2}\mathcal{G}_{0,2}^{2,0}\left(\frac{x}{4}\middle|\frac{\alpha}{2},-\frac{\alpha}{2}\right)$ [42, Eq. (03.04.26.0009.01)] within the integral \mathcal{I}_1 in (28), and then simplifying the integral by using [42, Eq. (07.34.21.0081.01)], we can get \mathcal{I}_1 as

$$\mathcal{I}_1 = \frac{\sqrt{\pi}}{32\alpha_{\text{RD}}^3\alpha_{\text{SR}}^2}G_{4,2:2,0:2,0}^{0,4;-0,5,-0,5,0,5,0,5}\left(-0,5,-0,5,0,5,0,5\middle|2,1\middle|0,5,-0,5\middle|\frac{\alpha_{\text{RD}}^2}{4\alpha_{\text{SR}}^2},\frac{\alpha_{\text{RE}}^2}{4\alpha_{\text{SR}}^2}\right).
 \tag{29}$$

Moreover, using $(\mathcal{K}_\alpha(\sqrt{x}))^2 = \frac{\sqrt{\pi}}{2}\mathcal{G}_{1,3}^{3,0}(x\middle|0,\alpha,-\alpha)$ [45, Eq. (8.4.23.27)], and [42, Eq. (03.04.26.0009.01)] within the integral \mathcal{I}_2 in (28), and then with the aid of [42, Eq. (07.34.21.0081.01)], we can obtain \mathcal{I}_2 as

$$\mathcal{I}_2 = \frac{\sqrt{\pi}}{32\alpha_{\text{RD}}^3\alpha_{\text{SR}}^2}G_{3,1:0,2:0,2}^{0,3;-0,1,1}\left(0,-1,1\middle|2,1\middle|0,0\middle|\frac{\alpha_{\text{RD}}^2}{4\alpha_{\text{SR}}^2},\frac{\alpha_{\text{RE}}^2}{4\alpha_{\text{SR}}^2}\right).
 \tag{30}$$

Substituting (29) and (30) into (28), we can obtain the intercept probability for variable gain relaying, $\mathcal{P}_{\text{int}}^v$, as presented in (14).

Appendix 2: Proof of Theorem 2

We can restructure \bar{C}_D^f in (19) as

$$\bar{C}_D^f = \underbrace{\mathbb{E}\left[\ln\left(1 + (1 + \lambda_{\text{SR}})\frac{\lambda_{\text{RD}}}{C}\right)\right]}_{\triangleq \mathcal{I}_1} - \underbrace{\mathbb{E}\left[\ln\left(1 + \frac{\lambda_{\text{RD}}}{C}\right)\right]}_{\triangleq \mathcal{I}_2}.
 \tag{31}$$

We first evaluate \mathcal{I}_1 as

$$\mathcal{I}_1 = \int_0^\infty \left[\int_0^\infty \ln\left(1 + \frac{(1+y)x}{C}\right) f_{\lambda_{\text{RD}}}(x) dx \right] f_{\lambda_{\text{SR}}}(y) dy.
 \tag{32}$$

Making the change of variable $\alpha_{\text{RD}}^2x = t$, and using [42, Eq. (01.04.26.0003.01)] and [41, Eq. (7.821.3)], the integral inside the square brackets can be expressed as

$$\mathcal{I}_1 = \int_0^\infty \left[G_{4,2}^{1,4}\left(\frac{1+y}{\alpha_{\text{RD}}^2 C}\middle|0,0,1,1\right) \right] f_{\lambda_{\text{SR}}}(y) dy.
 \tag{33}$$

Invoking the PDF of λ_{SR} into (33), and solving the integral with the help of $\mathcal{K}_\alpha(\sqrt{x}) = \frac{1}{2}G_{0,2}^{2,0}\left(\frac{x}{4}\middle|\frac{\alpha}{2}, \frac{-\alpha}{2}\right)$ [42, Eq. (03.04.26.0009.01)] and [42, Eq. (07.34.21.0082.01)], we obtain

$$\mathcal{I}_1 = \alpha_{SR}^2 \alpha_{RD}^2 C \sum_{k=0}^{\infty} \frac{1}{k!} \left(\frac{-1}{C\alpha_{RD}^2}\right)^k G_{3,7}^{6,2}\left(\alpha_{SR}^2 \alpha_{RD}^2 C \middle|_{0,0,k,k,k-1,k-1,k}^{0,k-1,k}\right). \tag{34}$$

Now, we can write \mathcal{I}_2 as

$$\begin{aligned} \mathcal{I}_2 &= \int_0^\infty \ln\left(1 + \frac{x}{C}\right) f_{\lambda_{RD}}(x) dx \\ &= \int_0^\infty \ln\left(1 + \frac{x}{C}\right) 2\alpha_{RD}^2 \mathcal{K}_0(2\alpha_{RD}\sqrt{x}) dx, \end{aligned} \tag{35}$$

which can be simplified using the fact that $\ln(1+x) = G_{2,2}^{1,2}(x|_{1,0}^{1,1})$ [42, Eq. (01.04.26.0003.01)], and making the change of variable $\alpha_{RD}^2 x = t$ and [41, Eq. (7.821.3)] as

$$\mathcal{I}_2 = G_{4,2}^{1,4}\left(\frac{1}{\alpha_{RD}^2} C \middle|_{1,0}^{0,0,1,1}\right). \tag{36}$$

Finally, invoking (34) and (36) into (31), we can obtain $\bar{\mathcal{C}}_D^f$ as

$$\begin{aligned} \bar{\mathcal{C}}_D^f &= \alpha_{SR}^2 \alpha_{RD}^2 C \sum_{k=0}^{\infty} \frac{1}{k!} \left(\frac{-1}{C\alpha_{RD}^2}\right)^k G_{3,7}^{6,2}\left(\alpha_{SR}^2 \alpha_{RD}^2 C \middle|_{0,0,k,k,k-1,k-1,k}^{0,k-1,k}\right) \\ &\quad - G_{4,2}^{1,4}\left(\frac{1}{\alpha_{RD}^2} C \middle|_{1,0}^{0,0,1,1}\right). \end{aligned} \tag{37}$$

Following the same steps as to obtain (37), we can get $\bar{\mathcal{C}}_E^f$ as

$$\begin{aligned} \bar{\mathcal{C}}_E^f &= \alpha_{SR}^2 \alpha_{RE}^2 C \sum_{k=0}^{\infty} \frac{1}{k!} \left(\frac{-1}{C\alpha_{RE}^2}\right)^k G_{3,7}^{6,2}\left(\alpha_{SR}^2 \alpha_{RE}^2 C \middle|_{0,0,k,k,k-1,k-1,k}^{0,k-1,k}\right) \\ &\quad - G_{4,2}^{1,4}\left(\frac{1}{\alpha_{RE}^2} C \middle|_{1,0}^{0,0,1,1}\right). \end{aligned} \tag{38}$$

Invoking (37) and (38) into (20), and after some algebraic simplifications, we can obtain the ESC under fixed gain relaying in (20).

Appendix 3: Proof of Theorem 3

Under variable gain relaying scenario, the ESC of the considered system can be expressed using (6) and (18) as

$$\begin{aligned}
 \bar{C}_{\text{SEC}}^v &= \frac{1}{2} \left\{ \mathbb{E} \left[\log_2 \left(1 + \frac{\lambda_{\text{SR}} \lambda_{\text{RD}}}{\lambda_{\text{SR}} + \lambda_{\text{RD}} + 1} \right) \right] - \mathbb{E} \left[\log_2 \left(1 + \frac{\lambda_{\text{SR}} \lambda_{\text{RE}}}{\lambda_{\text{SR}} + \lambda_{\text{RE}} + 1} \right) \right] \right\} \\
 &= \frac{1}{2 \ln(2)} \left\{ \underbrace{\mathbb{E}[\ln(1 + \lambda_{\text{RD}})]}_{\triangleq \mathcal{T}_1} - \underbrace{\mathbb{E}[\ln(1 + \lambda_{\text{RE}})]}_{\triangleq \mathcal{T}_2} - \underbrace{\mathbb{E}[\ln(1 + \lambda_{\text{SR}} + \lambda_{\text{RD}})]}_{\triangleq \mathcal{T}_3} \right. \\
 &\quad \left. + \underbrace{\mathbb{E}[\ln(1 + \lambda_{\text{SR}} + \lambda_{\text{RE}})]}_{\triangleq \mathcal{T}_4} \right\}. \tag{39}
 \end{aligned}$$

The terms \mathcal{T}_1 and \mathcal{T}_2 can be evaluated by using the fact that $\ln(1 + x) = G_{2,2}^{1,2}(x|_{1,0}^{1,1})$ [42, Eq. (01.04.26.0003.01)] and [41, Eq. (7.821.3)], as presented in (22) and (23), respectively.

Further, the term \mathcal{T}_3 can be expressed as

$$\begin{aligned}
 \mathcal{T}_3 &= \mathbb{E}[\ln(1 + \lambda_{\text{SR}} + \lambda_{\text{RD}})] \\
 &= \int_0^\infty \ln(1 + x) \left(\frac{\partial}{\partial x} \left(\int_0^x \int_0^{x-w} f_{\lambda_{\text{SR}}}(v) f_{\lambda_{\text{RD}}}(w) dv dw \right) \right) dx. \tag{40}
 \end{aligned}$$

By inserting the PDFs of λ_{SR} and λ_{RD} into (40), it is observed that the exact evaluation of (40) is intractable due to the involvement of two Bessel functions of different orders and arguments (e.g., $\mathcal{K}_m(\sqrt{x})\mathcal{K}_n(\sqrt{x-y})$). Therefore, for a tractable analysis, we can split the triangular integral region of $\lambda_{\text{SR}} + \lambda_{\text{RD}}$ into M rectangular subregions [40, 46], and slightly modify them to express \mathcal{T}_3 as

$$\begin{aligned}
 \mathcal{T}_3 &\approx \int_0^\infty \ln(1 + x) \left(\frac{\partial}{\partial x} \left(F_{\lambda_{\text{RD}}}\left(\frac{x}{M}\right) F_{\lambda_{\text{SR}}}(x) \right. \right. \\
 &\quad \left. \left. + \sum_{k=2}^M \left\{ \int_{x\tau_{k-1}}^{x\tau_k} f_{\lambda_{\text{RD}}}(v) dv \int_0^{x(1-\tau_{k-1})} f_{\lambda_{\text{SR}}}(w) dw \right\} \right) \right) dx \\
 &= \int_0^\infty \ln(1 + x) \left(\frac{\partial}{\partial x} \left(F_{\lambda_{\text{RD}}}\left(\frac{x}{M}\right) F_{\lambda_{\text{RD}}}(x) \right. \right. \\
 &\quad \left. \left. + \sum_{k=2}^M \left\{ (F_{\lambda_{\text{RD}}}(x\tau_k) - F_{\lambda_{\text{RD}}}(x\tau_{k-1})) F_{\lambda_{\text{SR}}}(x(1 - \tau_{k-1})) \right\} \right) \right) dx. \tag{41}
 \end{aligned}$$

It is worth noting that the expression in (41) is a good approximation to (40), which yields tight results over broad range of SNRs with negligible approximate error as M increases. Substituting the CDFs of λ_{SR} and λ_{RD} into (41) and using [45, Eq. (1.14.1.4)], we can express \mathcal{T}_3 as

$$\begin{aligned}
\mathcal{T}_3 \approx & \int_0^\infty \ln(1+x) \left[\frac{2\alpha_{RD}^2}{M} \mathcal{K}_0\left(2\alpha_{RD} \sqrt{\frac{x}{M}}\right) + 2\alpha_{SR}^2 \mathcal{K}_0(2\alpha_{SR} \sqrt{x}) \right. \\
& + \sum_{k=2}^M 2\alpha_{RD}^2 \left\{ -\tau_{k-1} \mathcal{K}_0(2\alpha_{RD} \sqrt{x\tau_{k-1}}) + \tau_k \mathcal{K}_0(2\alpha_{RD} \sqrt{x\tau_k}) \right\} \Big] dx \\
& + \int_0^\infty \ln(1+x) \left[-\frac{4\alpha_{SR}\alpha_{RD}^2 \sqrt{x}}{M} \mathcal{K}_0\left(2\alpha_{RD} \sqrt{\frac{x}{M}}\right) \mathcal{K}_1(2\alpha_{SR} \sqrt{x}) \right. \\
& - \frac{4\alpha_{SR}^2 \alpha_{RD} \sqrt{x}}{\sqrt{M}} \mathcal{K}_0\left(2\alpha_{RD} \sqrt{\frac{x}{M}}\right) \mathcal{K}_1(2\alpha_{SR} \sqrt{x}) \\
& + \sum_{k=2}^M \left\{ 4\alpha_{SR}^2 \alpha_{RD} (1-\tau_{k-1}) \sqrt{x\tau_{k-1}} \mathcal{K}_0(2\alpha_{SR} \sqrt{x(1-\tau_{k-1})}) \mathcal{K}_1(2\alpha_{RD} \sqrt{x\tau_{k-1}}) \right. \\
& + 4\alpha_{SR} \alpha_{RD}^2 \tau_{k-1} \sqrt{x(1-\tau_{k-1})} \mathcal{K}_1(2\alpha_{SR} \sqrt{x(1-\tau_{k-1})}) \mathcal{K}_0(2\alpha_{RD} \sqrt{x\tau_{k-1}}) \\
& - 4\alpha_{SR}^2 \alpha_{RD} (1-\tau_{k-1}) \sqrt{x\tau_k} \mathcal{K}_0(2\alpha_{SR} \sqrt{x(1-\tau_{k-1})}) \mathcal{K}_1(2\alpha_{RD} \sqrt{x\tau_k}) \\
& \left. \left. - 4\alpha_{SR} \alpha_{RD}^2 \tau_k \sqrt{x(1-\tau_{k-1})} \mathcal{K}_1(2\alpha_{SR} \sqrt{x(1-\tau_{k-1})}) \mathcal{K}_0(2\alpha_{RD} \sqrt{x\tau_k}) \right\} \right] dx. \tag{42}
\end{aligned}$$

where the first integral in (42) can be simplified with the help of [42, Eq. (01.04.26.0003.01)] and [41, Eq. (7.821.3)], whereas the second integral in (42) can be evaluated with the help of [42, Eq. (03.04.26.0009.01)], [42, Eq. (01.04.26.0003.01)], and [42, Eq. (07.34.21.0081.01)]. Consequently, after some algebraic manipulations, we can get \mathcal{T}_3 as given in (24).

Following the same approach as used to evaluate \mathcal{T}_3 in (24), we can get \mathcal{T}_4 as presented in (25).

References

1. Yan, G., & Rawat, D. B. (2017). Vehicle-to-vehicle connectivity analysis for vehicular ad-hoc networks. *Ad Hoc Networks*, 58, 25–35.
2. Hartenstein, H., & Laberteaux, K. P. (2008). A tutorial survey on vehicular ad hoc networks. *IEEE Communication Magazine*, 46(6), 164–171.
3. Martinez, F., Toh, C.-K., Cano, J.-C., Calafate, C., & Manzoni, P. (2010). Emergency services in future intelligent transportation systems based on vehicular communication networks. *IEEE Intelligent Transportation System Magazine*, 2(2), 6–20.
4. Akin, A. I., Ilhan, H., & Ozdemir, O. (2015). Relay selection for DF-based cooperative vehicular systems. *EURASIP Journal on Wireless Communications and Networking*, 30, 1–9.
5. Ahmed, E., & Gharavi, H. (2018). Cooperative vehicular networking: A survey. *IEEE Transactions on Intelligent Transportation Systems*, 19(3), 996–1014.
6. He, R., Molisch, A. F., Tufvesson, F., Wang, R., Zhang, T., Li, Z., et al. (2016). Measurement-based analysis of relaying performance for vehicle-to-vehicle communications with large vehicle obstructions. In *Vehicular technology conference (VTC-Fall), 2016 IEEE 84th* (pp. 1–6).
7. Sakiz, F., & Sen, S. (2017). A survey of attacks and detection mechanisms in intelligent transportation systems: VANETs and IoV. *Ad Hoc Networks*, 61, 33–50.
8. Parkinson, S., Ward, P., Wilson, K., & Miller, J. (2017). Cyber threats facing autonomous and connected vehicles: Future challenges. *IEEE Transactions on Intelligent Transportation Systems*, 18(11), 2898–2915.
9. Qu, F., Wu, Z., Wang, F. Y., & Cho, W. (2015). A security and privacy review of VANETs. *IEEE Transactions on Intelligent Transportation Systems*, 16(6), 2985–2996.

10. Hao, Y., Tang, J., & Cheng, Y. (2013). Secure cooperative data downloading in vehicular ad hoc networks. *IEEE Journal of Selected Areas in Communications*, 31(9), 523–537.
11. Raya, M., Papadimitratos, P., Aad, I., Jungels, D., & Hubaux, J.-P. (2007). Eviction of misbehaving and faulty nodes in vehicular networks. *IEEE Journal of Selected Areas in Communications*, 25(8), 1557–1568.
12. Asuquo, P., Cruickshank, H., Morley, J., Ogah, C. P. A., & Lei, A. (2018). Security and privacy in location-based services for vehicular and mobile communications: An overview, challenges, and countermeasures. *IEEE Internet Things Journal*, 5(6), 4778–4802.
13. Liu, Y., & Chen, H. H. (2017). Physical layer security for next generation wireless networks: Theories, technologies, and challenge. *IEEE Communication Surveys and Tutorials*, 19(1), 347–376.
14. Hamamreh, J. M., Furqan, H. M., & Arslan, H. (2018). Classifications and applications of physical layer security techniques for confidentiality: A comprehensive survey. *IEEE Communication Surveys and Tutorials*. <https://doi.org/10.1109/COMST.2018.2878035>.
15. Yener, A., & Ulukus, S. (2015). Wireless physical-layer security: Lessons learned from information theory. *Proceedings of the IEEE*, 103(10), 1814–1825.
16. Zou, Y., Zhu, J., Wang, X., & Hanzo, L. (2016). A survey on wireless security: Technical challenges, recent advances, and future trends. *Proceedings of the IEEE*, 104(9), 1727–1765.
17. Shiu, Y., Chang, S. Y., Wu, H., Huang, S. C., & Chen, H. (2011). Physical layer security in wireless networks: A tutorial. *IEEE Wireless Communications*, 18(2), 66–74.
18. Zou, Y., Wang, X., & Shen, W. (2013). Optimal relay selection for physical-layer security in cooperative wireless networks. *IEEE Journal of Selected Areas in Communications*, 31(10), 2099–2111.
19. Nguyen, B. V., & Kim, K. (2015). Secrecy outage probability of optimal relay selection for secure AnF cooperative networks. *IEEE Communication Letters*, 19(12), 2086–2089.
20. Yang, L., Chen, J., Jiang, H., Vorobyov, S. A., & Zhang, H. (2017). Optimal relay selection for secure cooperative communications with an adaptive eavesdropper. *IEEE Transactions on Wireless Communications*, 16(1), 26–42.
21. Fan, L., Lei, X., Duong, T. Q., Elkashlan, M., & Karagiannidis, G. K. (2014). Secure multiuser communications in multiple amplify-and-forward relay networks. *IEEE Transactions on Communications*, 62(9), 3299–3310.
22. Fan, L., Yang, N., Duong, T. Q., Elkashlan, M., & Karagiannidis, G. K. (2016). Exploiting direct links for physical layer security in multiuser multirelay networks. *IEEE Transactions on Wireless Communications*, 15(6), 3856–3867.
23. Wang, W., Teh, K. C., & Li, K. H. (2016). Relay selection for secure successive AF relaying networks with untrusted nodes. *IEEE Transactions on Information Forensics and Security*, 11(11), 2466–2476.
24. Kuehstani, A., Mohammadi, A., & Mohammadi, M. (2018). Joint relay selection and power allocation in large-scale MIMO systems with untrusted relays and passive eavesdroppers. *IEEE Transactions on Information Forensics and Security*, 13(2), 341–355.
25. Yang, M., Guo, D., Huang, Y., Duong, T. Q., & Zhang, B. (2016). Secure multiuser scheduling in downlink dual-hop regenerative relay networks over Nakagami-m fading channels. *IEEE Transactions on Wireless Communications*, 15(12), 8009–8024.
26. Zhao, R., Lin, H., He, Y. C., Chen, D. H., Huang, Y., & Yang, Y. (2018). Secrecy performance of transmit antenna selection for MIMO relay systems with outdated CSI. *IEEE Transactions on Communications*, 66(2), 546–559.
27. Sun, L., Ren, P., & Du, Q. (2014). Distributed source-relay selection scheme for vehicular relaying networks under eavesdropping attacks. *EURASIP Journal on Wireless Communications and Networking*, 109, 1–11.
28. Wang, D., Ren, P., Du, Q., Sun, L., & Wang, Y. (2017). Security provisioning for MISO vehicular relay networks via cooperative jamming and signal superposition. *IEEE Transactions on Vehicular Technology*, 66(12), 10732–10747.
29. Andersen, J. B. (2002, August). Statistical distributions in mobile communications using multiple scattering. In *Proceedings of the 27th URSI general assembly* (pp. 0090–6778).
30. Salo, J., El-Sallabi, H. M., & Vainikainen, P. (2006). Statistical analysis of the multiple scattering radio channel. *IEEE Transactions on Antennas and Propagation*, 54(11), 3114–3124.
31. Alghorani, Y., Kaddoum, G., Muhaidat, S., Pierre, S., & Al-Dhahir, N. (2016). On the performance of multihop-intervehicular communications systems over n^* Rayleigh fading channels. *IEEE Wireless Communications Letters*, 5(2), 116–119.
32. Seyfi, M., Muhaidat, S., Liang, J., & Uysal, M. (2011). Relay selection in dual-hop vehicular networks. *IEEE Signal Processing Letters*, 18(2), 134–137.

33. Nguyen, S. Q., & Kong, H. Y. (2016). Outage probability analysis in dual-hop vehicular networks with the assistance of multiple access points and vehicle nodes. *Wireless Personal Communications*, 87(4), 1175–1190.
34. Ilhan, H., Uysal, M., & Altunbas, I. (2009). Cooperative diversity for intervehicular communication: Performance analysis and optimization. *IEEE Transactions on Vehicular Technology*, 58(7), 3301–3310.
35. Xu, L., Huang, L., Cao, C., Wang, H., Li, Y., & Gulliver, T. A. (2018). Outage performance of mobile V2V cooperative networks. *Physical Communications*,. <https://doi.org/10.1016/j.phycom.2018.04.019>.
36. Ata, S. O., & Altunbas, I. (2016). Fixed-gain AF PLNC over cascaded Nakagami-m fading channels for vehicular communications. *AEU-International Journal of Electronics and Communication*, 70(4), 510–516.
37. Ai, Y., Cheffena, M., Mathur, A., & Lei, H. (2018). On physical layer security of double Rayleigh fading channels for vehicular communications. *IEEE Wireless Communication Letters*, 7(6), 1038–1041.
38. Zhang, J., & Pan, G. (2017). Secrecy outage analysis with Kth best relay selection in dual-hop inter-vehicle communication systems. *AEU-International Journal of Electronics and Communication*, 71, 139–144.
39. Pandey, A., & Yadav, S. (2018). Performance evaluation of amplify-and-forward relaying cooperative vehicular networks under physical layer security. *Transactions on Emerging Telecommunication Technologies*, 29(12), e3534.
40. Pandey, A., & Yadav, S. (2018). Physical layer security in cooperative AF relaying networks with direct links over mixed Rayleigh and double-Rayleigh fading channels. *IEEE Transactions on Vehicular Technology*, 67(11), 10615–10630.
41. Gradshteyn, I. S., & Ryzhik, I. M. (2000). *Table of integrals, series, and products* (6th ed.). Berlin: Academic Press.
42. The Wolfram Functions Site (Online). <http://functions.wolfram.com/>.
43. Brychkov, Y. A. (2008). *Handbook of special functions: Derivatives, integrals, series and other formulas*. London: CRC Press.
44. Mathai, A., & Saxena, M. R. K. (1973). *Generalized hypergeometric functions with applications in statistics and physical sciences*. New York: Springer.
45. Prudnikov, A. P., Brychkov, Y. A., & Marichev, O. I. (1990). *Integrals and series volume 3: More special functions*. London: Gordon and Breach Science Publishers.
46. Zhang, C., Ge, J., Li, J., Rui, Y., & Guizani, M. (2015). A unified approach for calculating the outage performance of two-way AF relaying over fading channels. *IEEE Transactions on Vehicular Technology*, 64(3), 1218–1229.

Publisher's Note Springer Nature remains neutral with regard to jurisdictional claims in published maps and institutional affiliations.



Anshul Pandey received the B.Tech. degree in Electronics and Communication Engineering from PDDM-Indian Institute of Information Technology Design and Manufacturing, Jabalpur, Madhya Pradesh, India, in 2012, and the M.Tech. degree in Advance Networks from ABV-Indian Institute of Information Technology and Management, Gwalior, India, in 2016. He is currently pursuing the Ph.D. degree with the Department of Electronics and Communication Engineering, Indian Institute of Information Technology Allahabad, Uttar Pradesh, India. His research interests include cooperative relaying for wireless vehicular networks, physical layer security, multiple-input-multiple-output communications, and signal processing.



Suneel Yadav received the B.Tech. degree in Electronics and Communication Engineering from Meerut Institute of Engineering and Technology, Meerut, India, in 2008, and the M.Tech. degree in Digital Communications from ABV-Indian Institute of Information Technology and Management, Gwalior, India, in 2012. He has completed his Ph.D. degree in the Discipline of Electrical Engineering at Indian Institute of Technology Indore, Madhya Pradesh, India, in 2016. He is currently with the Department of Electronics and Communication Engineering, Indian Institute of Information and Technology Allahabad, Uttar Pradesh, India, as an Assistant Professor. He has numerous publications in peer-reviewed journals and conferences. He is serving as a reviewer in a number of international journals including IEEE Transactions on Vehicular Technology, IEEE Communications Letters, IEEE Systems Journal, IEEE Access, and Transactions on Emerging Telecommunications Technologies. His current research interests are in the areas of wireless relaying techniques, cooperative communications, cognitive relaying networks, device-to-device com-

munications, signal processing, physical layer security, and MIMO systems.